

Fiber Formation and Characterization of a Thermotropic LCP

JUHA SARLIN and PERTTI TÖRMÄLÄ, *Tampere University of
Technology, Institute of Plastics Technology, P.O. Box 527,
SF-33101 Tampere, Finland*

Synopsis

Our work dealt with the spinnability of the commercial liquid crystal polymer Vectra A900 (Celanese Speciality Operations, Ltd.). The nonisothermal spinning was carried out using a pilot-plant scale equipment and a monofilament die. The mass flow rate was constant while take-up velocity was varied between 200 and 1100 m min⁻¹ and spinning temperature between 287 and 327°C. In the light of results it seems that the spin-draw ratio is of little importance insofar as it is over 30, albeit the best tensile strengths and modulus were obtained with the highest spin-draw ratio. The fibers showed the inhomogeneity in particular with high spinning temperatures. A SEM analysis of the fibers also showed that high spinning temperature is apt to produce defects in the fibers.

INTRODUCTION

As a result of intensive research into the synthesis of thermotropic liquid crystal polymers, the midseventies witnessed a boom in patent applications and a subsequent rise in the number of scientific reports published on the properties of these materials. The rigid rodlike molecules, which in the meso-phase have a low viscosity and high orientability, and the long relaxation times of polymers make these materials a viable alternative in the pursuit of high-strength fibers.¹ Previous research has mainly focussed on nematic main chain liquid crystalline polymers; in addition there have been some works concerned with the fiber formation of smectic side chain polymers.²

A material frequently discussed in published reports has been the PET/HBA copolymer. 4-Hydroxy-benzoic acid (HBA) polymer is as such a highly crystalline material that it does not submit to melt processing. The copolymer is melt processable and displays a liquid crystalline behavior.³⁻⁵ In the case of this material, the crystallinity of HBA and the related thermal and shear history have themselves produced a number of problems.⁶⁻¹⁰ The mechanical properties, then, are not the best possible either.¹¹ Despite the extensive research into this material, the development of commercial applications has proceeded to little avail.

Materials that have recently received much attention in research, mainly from the Hoechst Celanese Co., are naphthalenic-based copolymers containing HBA and 2-hydroxy-6-naphthoic acid (HNA).^{12,13} These materials have yielded some commercially promising results.

In addition to the above materials there are also a number of other thermotropic liquid crystalline polymers. HBA and HNA have proved rather useful

components; other materials commonly used with them are hydroquinone (HQ), isophthalic acid (IA), and terephthalic acid (TA). The development of thermotropic polymers is described in more detail, for example, in some excellent review articles.¹⁴⁻¹⁶

EXPERIMENTAL

Polymer

The raw material used in this work was Vectra A 900. The melting point given by the manufacturer is 280°C, and the previously measured T_g point is 97°C.^{17,18} Before spinning, the polymer was dried at a temperature of 120°C for 24 h. Melt rheology measurements were carried out in a Rheometrics equipment at a frequency of 1 Hz.

Spinning

The spinning was performed using a pilot-plant scale Fourné spinning machine. The screw diameter is 13 mm and the L/D ratio 24. The machine is equipped with a metering pump. The measured diameter of the used monofilament die was 1 mm.

The spinning took place under nonisothermal conditions, and no cooling air flow was directed to the fibers. The mass flow rate was constant, $W = 4.45 \text{ g min}^{-1}$. Take-up speed V_L was adjusted to attain the desired spin-draw ratio. The used V_L rates were 200, 400, 600, 800, and 1100 m min^{-1} . Three spinning temperatures were used, 287, 307, and 327°C. The lowest spinning temperature was selected on the basis of preliminary works carried out on a piston extruder which showed the fragility of the melt when T_S was below 285°C.

The take-up device was composed of two godets and a bobbin. The speeds of each part could be controlled separately, and the godets were adjusted to rotate slightly slower than the bobbin. This arrangement forms a slight tension in the fiber coil and ensures proper take-up. The difference in speeds also produces a degree of friction between the fiber and the godets. To reduce this friction, a small amount of water was sprayed on the surfaces of the godets.

The tension of the fiber was measured by a Rothschild Electronic Tensiometer R-3192. The measuring head size was 10 cN and the device was calibrated in conformity with the manufacturer's instructions. The measuring head was located immediately before the first godet. The measuring signal of the tensiometer was recorded using a y-t recorder.

Fiber Diameter

The fiber diameter D_f was determined on the basis of linear density. The density value used is that given by the manufacturer, $\rho = 1.38 \text{ g cm}^{-3}$.¹⁷ The fiber diameter thus obtained was identical to the values measured on an optical microscope. The spin-draw ratio $\Gamma = A_0/A_f$ was determined on the basis of the diameters of capillary, D_0 , and fiber, D_f .

There are many ways to measure a fiber profile. Instead of the fiber diameter the fiber speed can be measured using laser-Doppler velocimetry.¹⁹ The common ways also include on-line measurement with an optical microscope, photography,

or using a special cutter to get a piece of the fiber.²⁰⁻²² Here the fiber was cut about 2 m below the die and immediately after that straight below the die. This method cannot be considered as sophisticated as the above methods; nevertheless, observations made earlier during this study lend support to the current results. As the extrudate flowing from the die after the lower cut was no longer under elongational tension, it was not possible to determine the location of the die directly on the basis of specimen length. The starting point of elongation, in other words, the location of the die exit at the time of the lower cut, was determined as the point where the fiber thickness became constant. The specimen was then cut into pieces of 50 mm and placed on a microscopic slide, and the thicknesses were measured at intervals of 5 mm with the aid of the specimen holder micrometer. The drawback of this way of determining the fiber profile lies in the potential deformation involved in the sampling at the threadline, but, in the light of the previous observations made, the results can be considered rather reliable.

The material testing was performed on a JJ M30K type universal material testing machine. Specimen length l_0 was 50 mm and the crosshead speed was 5 mm min^{-1} . In general the l_0 is 1 in. or less. However, as the tensile strength correlates with specimen length, i.e., the probability of attaining high strength values increases with decreasing l_0 values, we used quite high l_0 values to minimize this effect.²³ The material testing machine automatically printed the crosshead travel to the fracture point and the maximum force attained. This crosshead travel was used to determine the tensile elongation ϵ_b and the maximum force to determine the ultimate tensile strength σ . The force was recorded on a y-t recorder, and the stress-strain curve was used to determine initial modulus E . The results of the material testing were the averages of a minimum of 10 specimens.

Fiber structures were examined on an ISI 40 scanning electron microscope.

RESULTS

Storage modulus G' , loss modulus G'' , and complex viscosity η^* at a temperature range of 300–325°C showed a drastic decrease starting at a temperature of approx. 305°C (Fig. 1). Although the measurement does not cover the lowest spinning temperature 287°C, in the light of the curves it seems that in this case the dynamic properties of the melt are largely similar as at the low-temperature end.

Threadline Properties

An outstanding advantage of the material seems to be that it yields high spinnability, in particular at low spinning temperatures. Temperatures exceeding 310°C caused a drastic reduction in the melt strength, which made it rather difficult to obtain high spin-draw ratios. The reduction in fiber diameter took place over a short distance. When T_s was 287°C, and the spin-draw ratio was 190, the fiber reached its final diameter at a distance of 435 mm from the die exit. When the spinning temperature increased 307°C, the distance needed for the elongation decreased to 390 mm (Fig. 2). This acceleration of deformation with increasing temperatures is similar to that observed in conventional

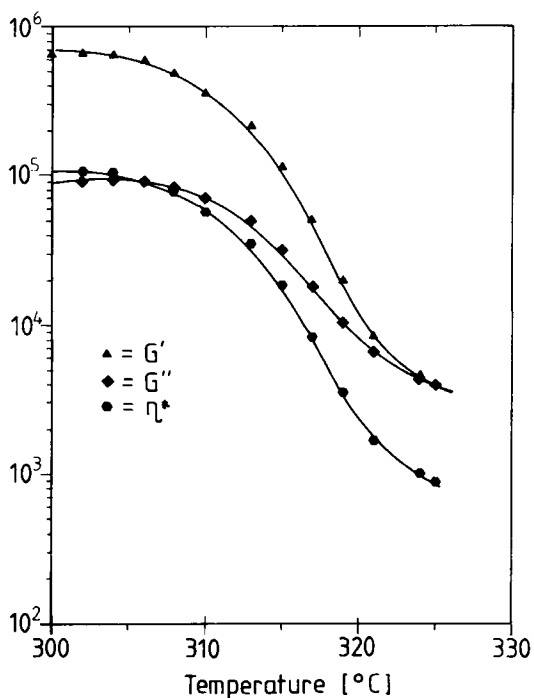


Fig. 1. Storage modulus G' (Pa), loss modulus G'' (Pa), and complex viscosity η^* of melt.

polymers. A closer look at Figure 2 reveals considerable oscillation in the fiber profile with the higher spinning temperature. The obvious explanation lies in the inhomogeneity discussed later in this paper.

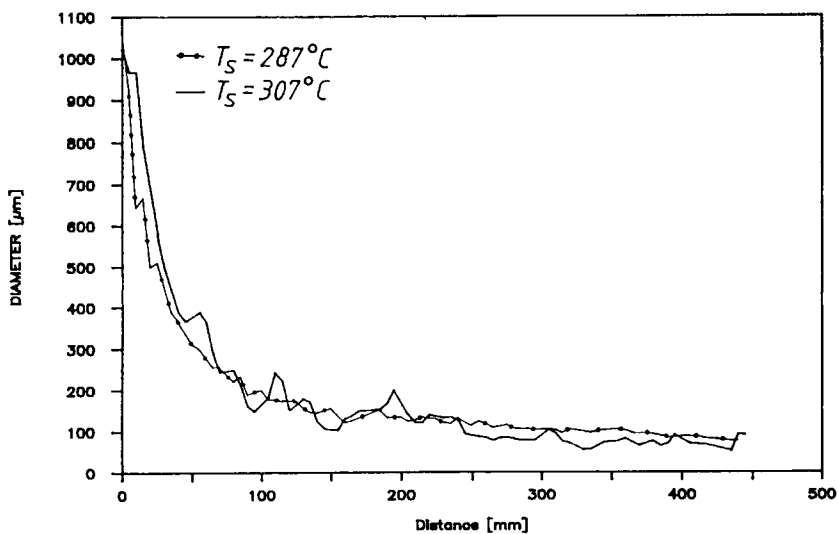


Fig. 2. Fiber profile after die exit at spinning temperatures of 287 and 307°C, spin-draw ratio is 190 in both cases.

While measuring the fiber profile to determine the point where elongation had stopped when the fiber was cut, it was noticed that the constant maximum fiber diameter before the elongation zone (the extrudate diameter) was greater than the capillary diameter, which suggests a die swell. At temperatures of 287 and 307°C, D_0 were 1065 and 1022 μm , respectively. These values correspond to swelling ratios 1.31 and 1.26, respectively. However, it should be noted here that this is not a reliable method for measuring the die swell effect.

There is virtually no comparable data available on the die swell phenomenon; previous observations mainly concern the PET/HBA copolyester, in particular, the PET/60HBA polymer.^{9,24-26} Done and Baird submerged a capillar end in oil, thus cooling the extrudate quickly, and observed a clear die swell behavior with PET/60HBA, PET/80HBA, and LCP2000. The phenomenon disappeared when the rapid cooling was no longer used. LCP2000 was an early naphthalenic-based liquid crystalline polymer of Celanese, and evidently to some extent similar to the polymer used in this study. The die swell ratio for the LCP2000 was about 1.4 compared with 1.02 for the chase without quenching the exit.

There was a considerable reduction in the take-up force F_{ex} measured from the fiber when T_S increased from 287 to 307°C. The F_{ex} measured at the lower temperature was 3.3 cN as compared to 1.9 at the higher temperature. The spin-draw ratio for both cases is 190. Comparing the change of F_{ex} as a function of temperature against the change of the dynamic properties of the melt brings out a clear correlation. The spinning tension consists of five factors, air-drag force F_{air} , gravitational force F_{grav} , inertia force F_{in} , rheological force F_{rheo} , and surface tension F_{surf} . The measurable quantity, take-up force F_{ex} is the sum total of these five terms. As F_{grav} and F_{surf} are generally negligible, and at slow speeds F_{in} is also low, then in practice F_{ex} is the sum of F_{rheo} and F_{aero} only. Ziabicki has presented that, in the case of PET and a V_L value 1000 m min^{-1} , F_{ex} in practice consists of almost equal F_{rheo} and F_{aero} .²⁷ Here the F_{aero} is virtually constant, and thus the measured change is attributable solely to the change in the elongational viscosity of the polymer. This implies problems in spinning with further increasing of spinning temperature.

Some oscillation was observed in the fiber tension (Fig. 3). At the lower spinning temperature relatively long-term oscillation is observed. A probable explanation for this is a slight oscillation in the operation of the metering pump, which in turn is attributable to the fact that the equipment was designed for multifilament spinning, but this time it was used with a monofilament die. This arrangement made it necessary to use a very low rotation speed, reflected in a slight variation in the running visible in the tachometer reading. No variation could be observed in the speed of the take-up equipment.

At the higher temperature the above long-term oscillation could hardly be observed, but instead there was a very short-term oscillation. One explanation may lie in the previously mentioned variation in fiber diameter, which, due to the method of measurement used, is reflected in a variation in force. If this were the case, the tension measurement would prove that the fiber diameter would not be as constant in the higher temperature as in the lower.

Tensile Properties

There is a slight increase in the modulus when the spin-draw ratio increases from the lowest value of 30–70 (Fig. 4). At the lowest spin-draw ratio the

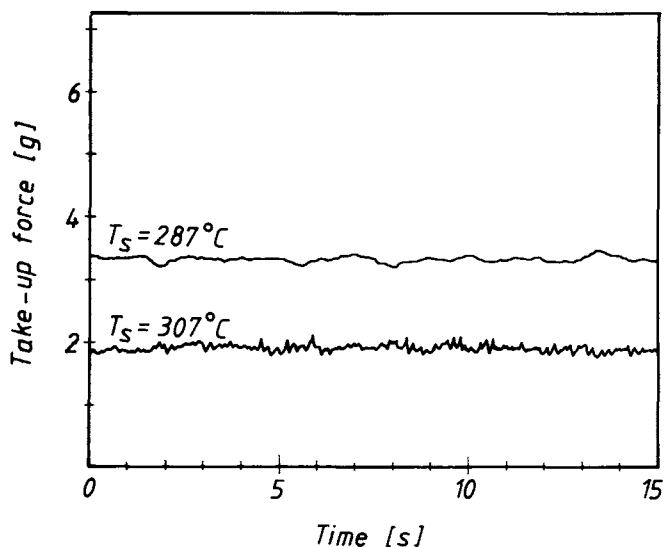


Fig. 3. Spinning tension, when $T_S = 287$ and 307°C and the spin-draw ratio is 190.

modulus is in practice independent of the spinning temperature. Likewise, at a spin-draw ratio of 70 spinning temperature has little effect. When T_S is 287°C , increasing the spin-draw ratio does not affect the modulus to a significant degree, albeit the highest modulus, 60 GPa, is attained with this lowest spinning temperature and with the highest spin-draw ratio. When T_S was 307°C , a rising Γ does not essentially affect the modulus with the exception of the smallest spin-

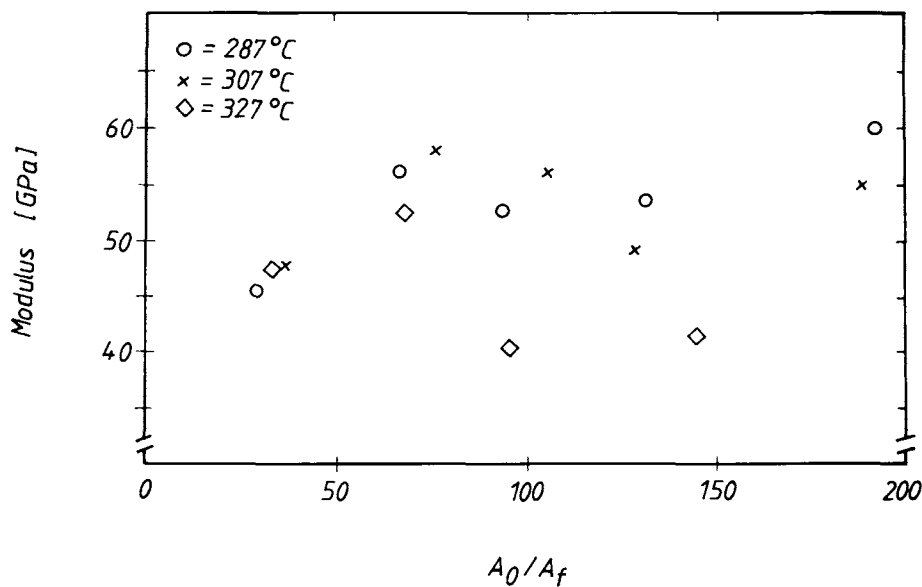


Fig. 4. Tensile modulus vs. spin-draw ratio.

draw ratio. Thus the structure development must be very rapid. At the highest spinning temperature E decreases significantly when Γ exceeds 70.

Previously published results have generally noted that attaining a high modulus does not require using especially high spin-draw ratios. Kenig has noted that with many LCP materials spin-draw ratios under 10 are sufficient for attaining almost the maximum modulus.²⁸ Ide and Ophir have noted that with HBA/HNA/TA polymers the modulus in practice reaches a maximum at a spin-draw ratio of about 50.²⁹ According to the results of Muramatsu and Krigbaum a spin-draw ratio of 10 used with PET/60HBA yielded the maximum modulus.⁷ Tealdi et al. noted that, with PET/60HBA copolymer a rising tendency in the modulus with growing spin-draw ratios, the rise turned down at a spin-draw ratio of 150.⁶ Raising the spinning temperature, according to Acierno et al.,¹¹ seems with PET/60HBA to decrease the modulus. On the other hand, the results of Muramatsu and Krigbaum show exactly the opposite: A higher spinning temperature yields a higher modulus. Yet in a later study they repeated the test with a new specimen and found spinning temperature to have no significant effect on the modulus.⁸ Cuculo and Chen have also noted the modulus to increase with an elevation of the spinning temperature.³⁰ Underlying this discrepancy is the crystallinity of HBA in the PET/HBA polymer. This sensitivity of PET/HBA to thermal history is also clearly evidenced by Tealdi et al. Calundann and Jaffe have proposed the modulus of a naphthalenic-based LCP to develop with the spin-draw ratio and to reach a maximum at a ratio of about 30, which agrees well with the results obtained in this study.¹⁶

A slight increase can be observed in the tensile strength with increasing spin-draw ratios when the spinning temperatures are 287 and 307°C (Fig. 5). The lower spinning temperature yield slightly better strength values with the maximum reached at 1.2 GPa, at the highest spin-draw ratio. At the highest

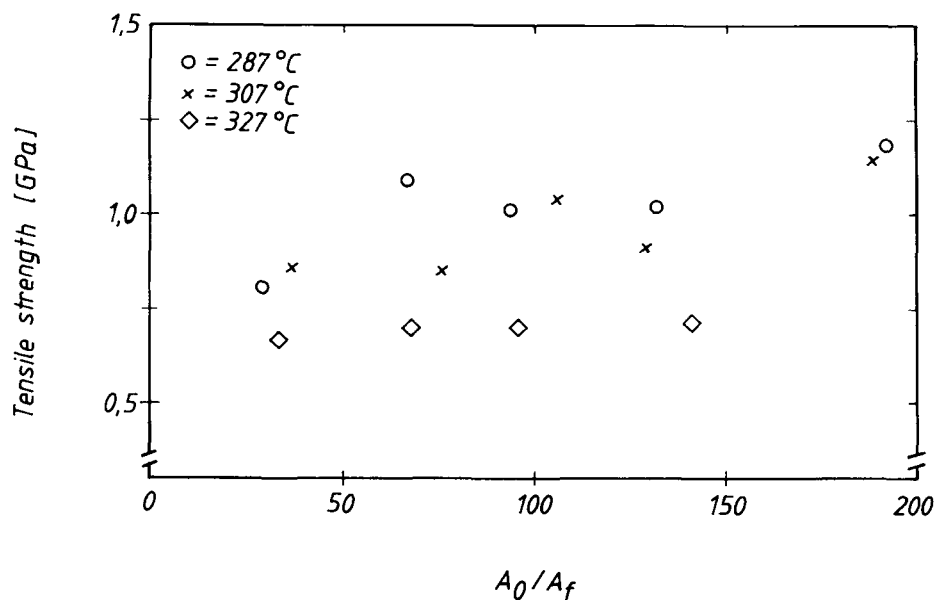


Fig. 5. Tensile strength vs. spin-draw ratio.

T_S the tensile strength is independent of the spin-draw ratio; the strength is also considerably lower than at lower spinning temperatures.

There are less comparable results available on tensile strengths than on the modulus. Cuculo and Chen obtained almost a linear correlation between the tensile strength of PET/60HBA and the spin-draw ratio. According to the results of Cuculo and Chen, the temperature had a similar effect on the strengths as on the modulus; i.e., the strength increased with increasing spinning temperatures. Calundann and Jaffe have also reported results that agree with the results obtained in our work.

The elongation at break is almost independent of the spin-draw ratio (Fig. 6), by contrast, decreasing the spinning temperature reduces the elongation at break. At the lowest spinning temperature ϵ_b is about 2.4% and at the highest spinning temperature about 1.8%. The cause can be traced back to the previously mentioned inhomogeneity, i.e., high levels of inhomogeneity add result in a low elongation at break when the fracture takes place at local tension maximums.

For a PET/60HBA copolymer Acierno et al. have obtained almost a constant value for elongation at break, about 1.5%, although the results contain a local maximum. Likewise, Calundann and Jaffe observed break elongations exceeding 5% at low spin-draw ratios, although the elongation decreased rapidly to a little over 2% when the spin-draw ratio approached 50; after this point the elongation was no longer affected by the growth of the spin-draw ratio. Here the results obtained in the present study and the above-mentioned study were well in agreement.

SEM

The general impression in the SEM analysis was that the fiber structure was rather homogeneous at the lowest spinning temperature, and no actual

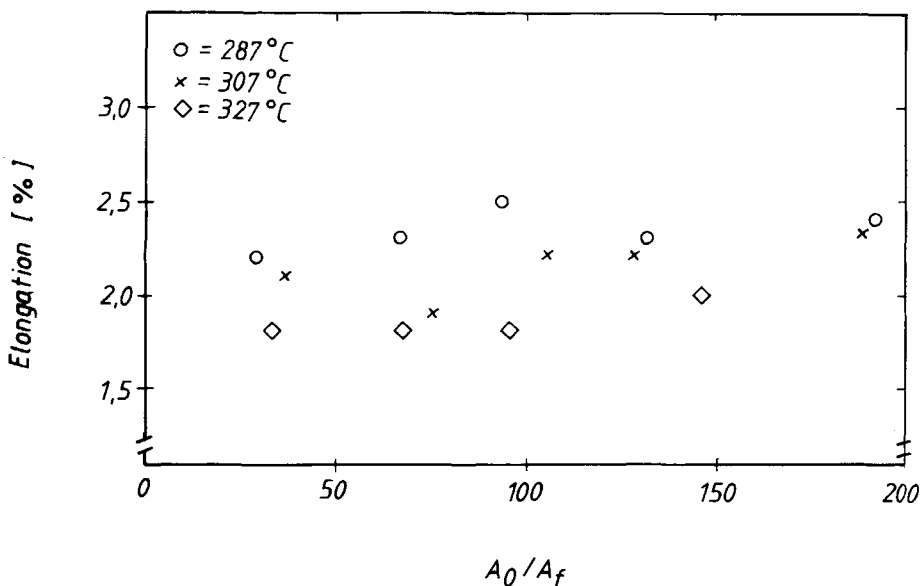


Fig. 6. Elongation at break against spin-draw ratio.

defects could be found. Figure 7 shows a photomicrograph of a fiber; T_S is 287°C and $\Gamma = 190$. The fiber surface was virtually defect-free and a clear macrofibrillar structure was visible. Sawyer and Jaffe have described this hierarchical structure of the fibrils rather accurately, although the phenomenon itself is not limited to LCP fibers.³¹ The fiber cross section was round. Figure 8 shows the same fiber in a picture produced using an enhanced signal; here the macrofibrillar structure and its regularity are evident. In the light of the SEM analysis it seems that the low spinning temperature produced a rather regular and defectless fiber structure. The observed defects were mainly peeling of fibrils as a result of frictional stress in the take-up and specimen preparation. This phenomenon is as such a major problem in view of the practical applications of fibers, where fibers are often subjected to frictional stresses.

With increasing spinning temperatures the SEM revealed a clear change in the fiber structure (Figs. 9 and 10). The fibers lost their round shape. The structure can be interpreted by the tendency of macrofibrils to form partly separate groups sometimes with distinct borders. It seems that these macrofibril groups are more sensitive to peeling than a more homogeneous fiber processed at a lower spinning temperature. Detached fibrils and even bunches of fibrils were quite common in these specimens. The origin of these detached fibrils lies in the spinning process itself, mainly the take-up. The specimens were cut from the original coil with extreme care, thus the loose fibrils could not originate in the processing of the specimen.

As the spinning temperature increases to 327°C , cracklike defects appear between the macrofibril groups; an example is Figure 11.

INHOMOGENEITY

As was already noted, some inhomogeneity can be observed in the fiber diameter. This phenomenon is less pronounced at low T_S values, but at higher spinning temperatures the inhomogeneity reaches a significant level. The phenomenon grows more pronounced with an increase in the spin-draw ratio. The diameter of the fiber, $T_S = 327^\circ\text{C}$ and $\Gamma = 146$, is measured at intervals of 50 mm, and the results are presented in Figure 12. The strong variation in the diameter is visible in the picture. The variation is not completely regular; nevertheless, a rough basic frequency of approx. 30 cm can be perceived in the picture. In the spinning the frequency of this oscillation, measured on the basis of V_L (800 m min^{-1}), is approx. 44 Hz and in relation to V_0 it is about 0.2 Hz. There are several possible origins for this inhomogeneity. One possible cause would be the uneven running of the machine, i.e., variation either in mass flow rate or in take-up velocity. The slight oscillation in the speed of the metering pump has already been mentioned, but the frequency of the variation precludes this possibility, because the metering pump oscillation is much slower. Besides, the intensity of the variation does not correlate with the pump oscillation. On the other hand, no oscillation has been observed in the take-up speed, and the high intensity of the observed variation would require considerable variation in the speed of rotation. The oscillation frequency would also be lower. The phenomenon was also observed in preliminary tests on a piston extruder. Now it is evident that the low strengths measured with higher spinning temperatures result from the observed inhomogeneity.

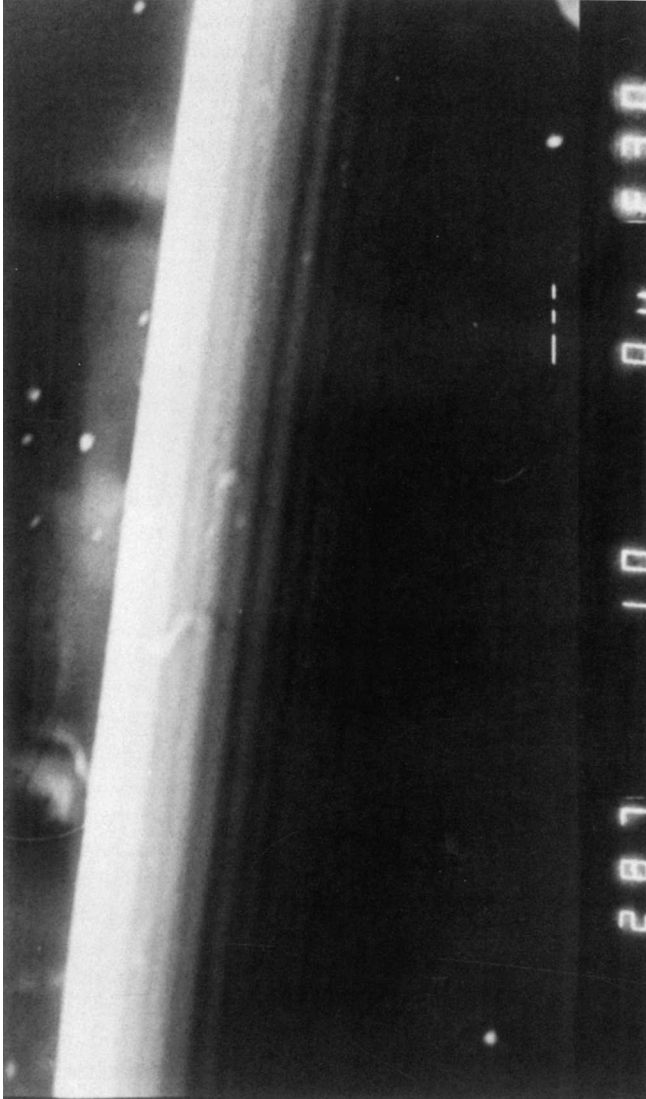


Fig. 7. SEM photomicrograph of fiber, $T_s = 287^\circ\text{C}$ and spin-draw ratio 190. Scale bar length is $10\ \mu\text{m}$ in all graphs.

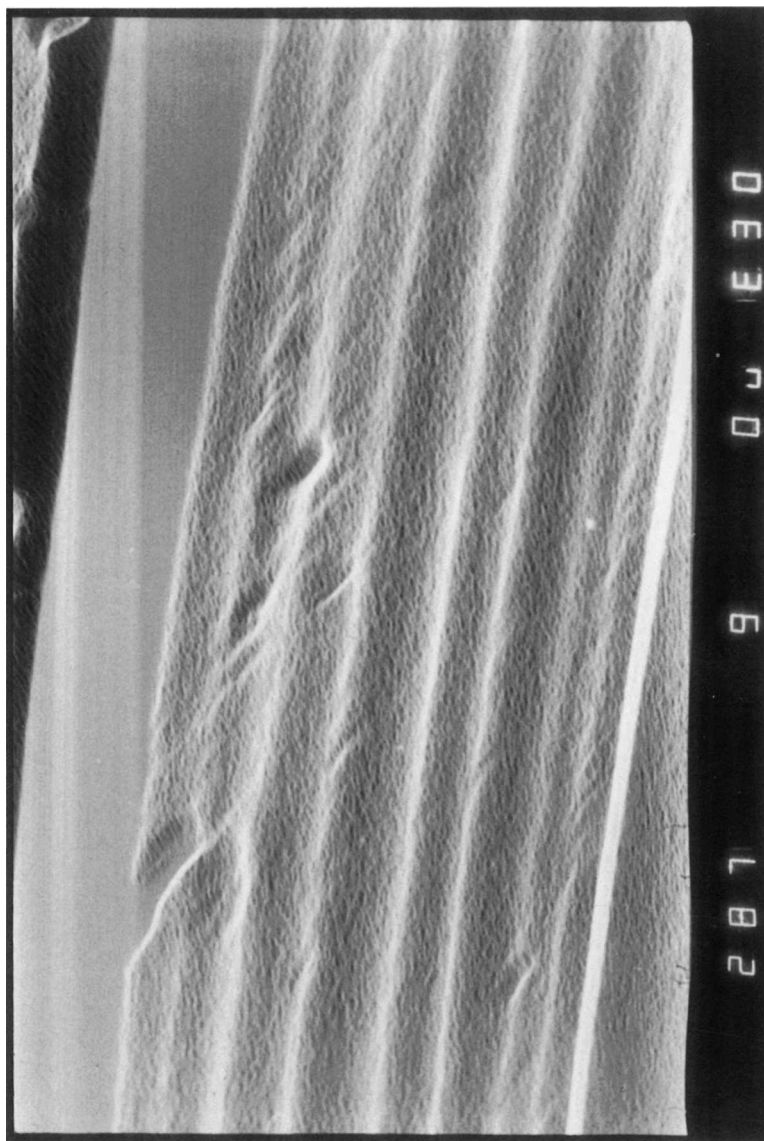


Fig. 8. Micrograph produced by signal derivation, same fiber as above.

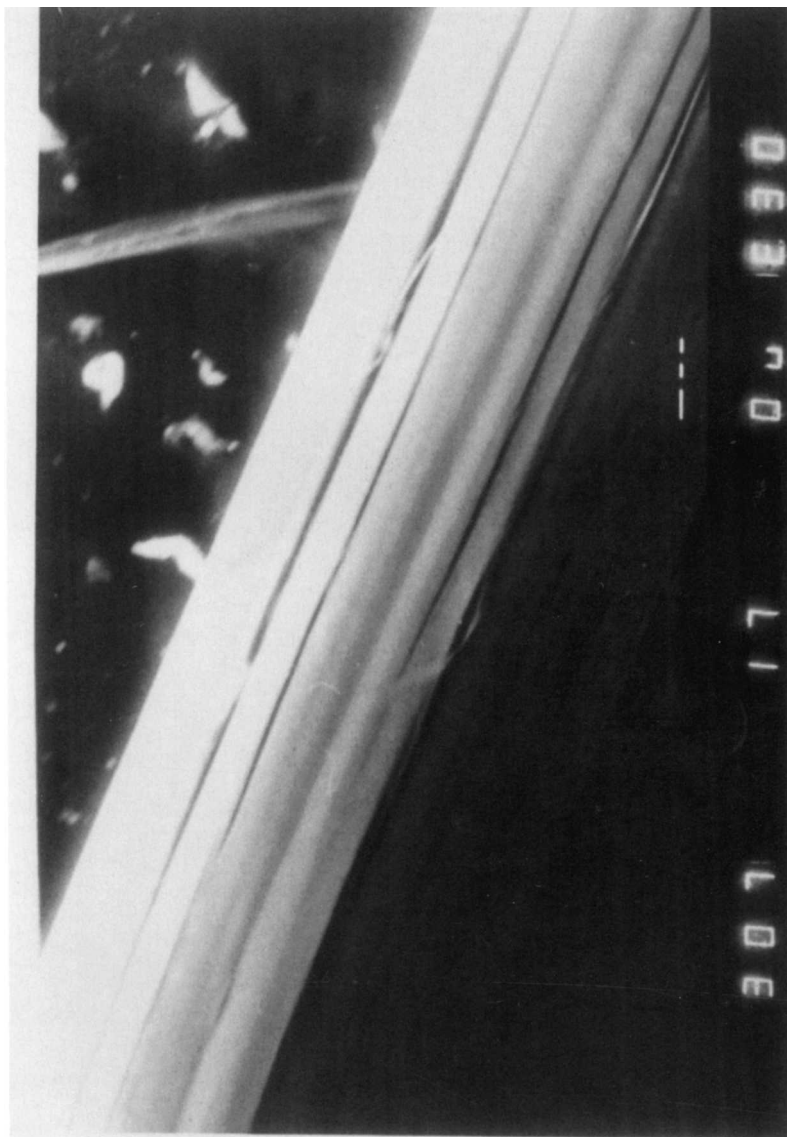


Fig. 9. SEM photograph of fiber, $T_s = 307^\circ\text{C}$ and spin-draw ratio about 100.

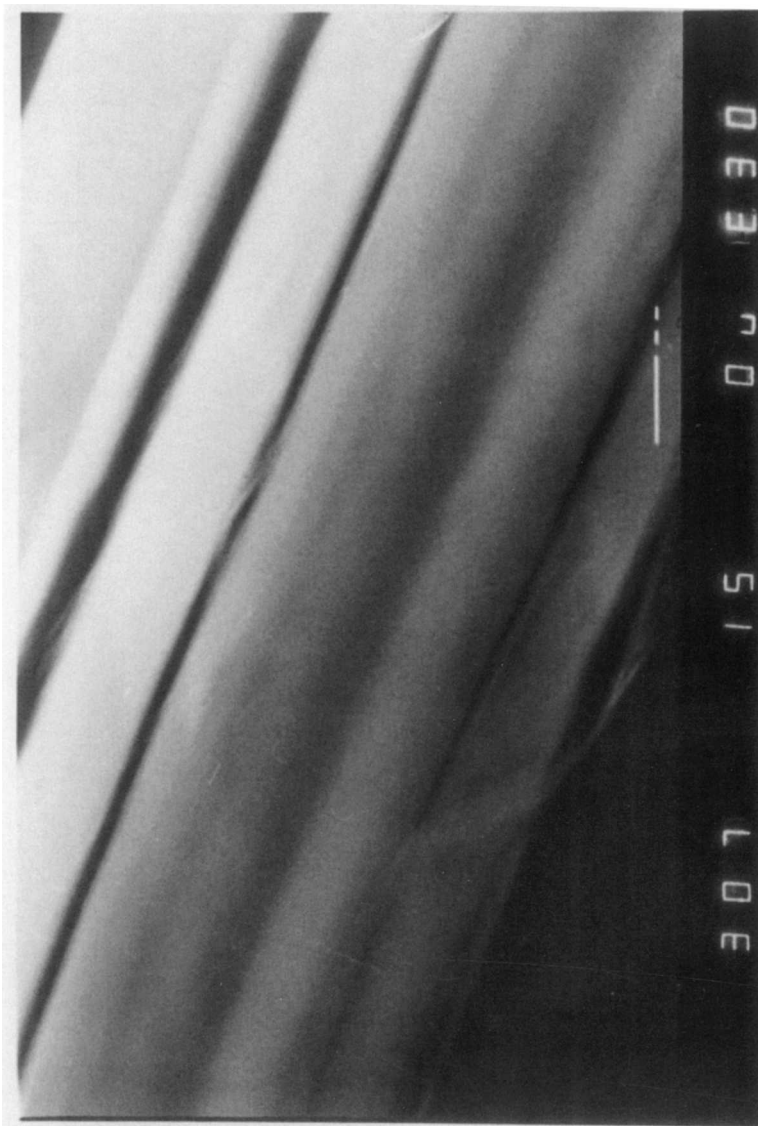


Fig. 10. Same fiber as above, larger magnification.

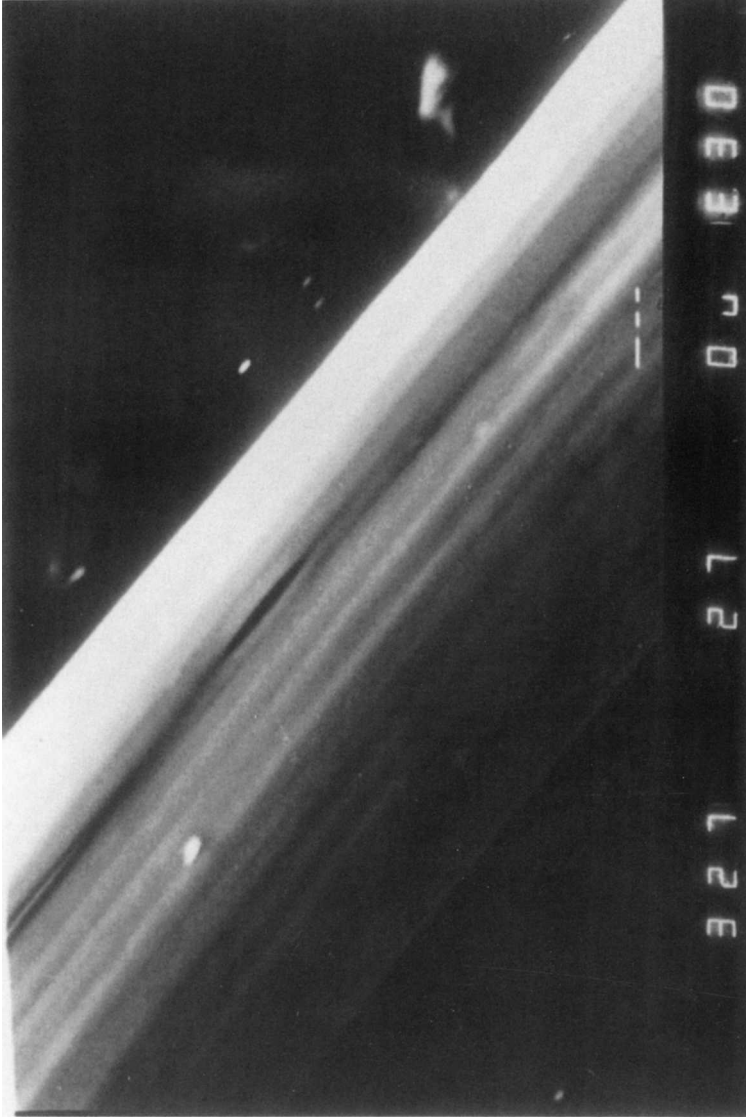


Fig. 11. SEM photograph of fiber, $T_s = 327^\circ\text{C}$ and spin-draw ratio 146.

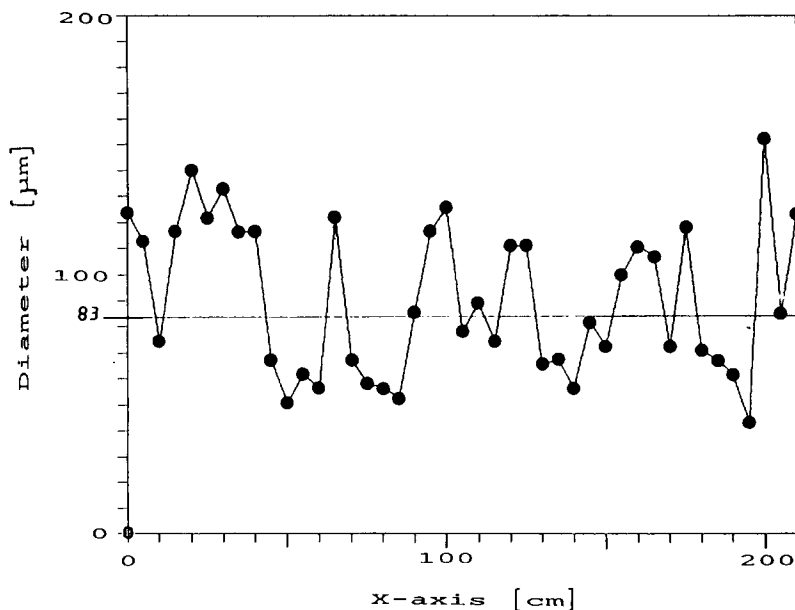


Fig. 12. Variation of fiber thickness measured at intervals of 5 cm, $T_s = 327^\circ\text{C}$, and spin-draw ratio 146.

One possible source of inhomogeneity would also be the inhomogeneity of the melt. The variation in the polymer viscosity could result from inadequate homogenization of the melt, although an extruder equipped with a metering pump should ensure a rather homogeneous melt. Another possible source is inhomogeneity in the raw material.

A third possible source of inhomogeneity would be drawn resonance. It implies a regular oscillation in the fiber diameter; the frequency and amplitude of this oscillation would be affected by the properties of the material and by processing conditions.³²⁻³⁵ This phenomenon stems from an instability in the threadline that can only emerge when the spin-draw ratio exceeds 20 in the case of Newtonian fluids; in the case of non-Newtonian fluids the critical spin-draw ratio is still lower.³⁶ Verifying this possibility would require an extensive analysis, which has not been within the scope of this study. Metzner and Prilutski have observed a tendency of liquid crystalline polymers towards instability during spinning.³⁷

Krigbaum has observed a similar instability in fibers and deduced this instability to be a result of a network formed by HBA crystallites.³⁸

CONCLUSIONS

As a whole the polymer yielded promising spinning results, especially at low spinning temperatures, which permitted using high spin-draw ratios. It is also worth noting that this study revealed no probable obstacles to using higher spinning speeds than the maximum speed used here. This is almost inevitable, if the process is to be scaled up to industrial scale.

As the mass flow rate remained constant through the study, it is not possible to state the effect of the shear rate on the fiber properties, although it has been noted that a higher shear rate improves the properties of as-spun fibers. At the spinning speed range used the spin-draw ratio does not have any essential importance, although the maximum values for strength and modulus (1.2 and 60 GPa) were obtained at the highest spin-draw ratio.

On the other hand, the changes observed in previous publications have occurred at lower spin-draw ratios than the lowest ratio used here. The spinning temperature, by contrast, turned out to be an essential processing parameter. There is no doubt that the best mechanical properties were obtained at a low spinning temperature. The observed inhomogeneity in the fiber diameter was enhanced at high spinning temperatures. Measurements of fiber spinning tension and profile for their part suggested that raising the spinning temperature may cause inhomogeneity. An examination of the fiber surface also brought out the increase in defects with higher spinning temperatures. Yet it is not possible on the basis of this study to draw any unambiguous conclusions covering all the factors that deteriorated fiber properties at high T_S values. In general, the mechanical properties attained were rather similar to those obtained by Calundann and Jaffe, which suggests some similarities between the materials used in this study and their material.

The authors gratefully acknowledge Mr. Åke Henriksson, who gave us an opportunity to use the spinning equipment, and Mr. Ilpo Pyykkö for his valuable help in the practical spinning, both of them from the Tampere University of Technology, Institute of Textile Technology. We are grateful to Mrs. Eeva-Leino Heino of Neste Ltd. for carrying out the melt rheology measurements. We would also like to thank Ms. Outi Anttila for her careful work in performing the material testing.

APPENDIX: NOMENCLATURE

| | |
|-------------------|---|
| A_0 | cross-sectional area of capillary (mm^2) |
| A_f | cross-sectional area of fiber (mm^2) |
| D_0 | diameter of capillary (mm) |
| D_f | diameter of fiber (μm) |
| E | initial modulus (GPa) |
| F | axial tension (N) |
| F_{aero} | skin-friction contribution to spinning line tension (N) |
| F_{grav} | gravitational contribution to spinning line tension (N) |
| F_{in} | inertial contribution to spinning line tension (N) |
| F_{ext} | take-up force (cN) |
| F_{rheo} | rheological contribution to spinning line tension (N) |
| F_{surf} | surface tension contribution to spinning line tension (N) |
| G' | storage modulus (Pa) |
| G'' | loss modulus (Pa) |
| x | distance from spinneret (mm) |
| l_0 | sample length (mm) |
| T_S | spinning temperature ($^{\circ}\text{C}$) |
| V_L | take-up velocity (m min^{-1}) |
| W | mass outflow (g min^{-1}) |
| ϵ_b | elongation at break (%) |
| η^* | complex viscosity (P) |
| ρ | density (g cm^{-3}) |
| σ | tensile strength (GPa) |

Γ spin-draw ratio
 χ die swell ratio

References

1. W. J. Jackson, Jr., *Macromolecules*, **16**, 1027 (1983).
2. P. Zugenmaier, *Makromol. Chem., Suppl.*, **6**, 31 (1984).
3. G. Lieser, G. Swarz, and H. R. Kricheldorf, *J. Polym. Sci. Polym. Phys. Ed.*, **21**, 1599 (1983).
4. G. Lieser, *J. Polym. Sci. Polym. Phys. Ed.*, **21**, 1611 (1983).
5. J. Economy, R. S. Storm, V. I. Matkvich, S. G. Cottis, and B. E. Nowak, *J. Polym. Sci. Polym. Chem. Ed.*, **14**, 2207 (1976).
6. A. Tealdi, A. Ciferri, and G. Conio, *Polymer Commun.*, **28**, 22 (1987).
7. H. Muramatsu and W. R. Krigbaum, *J. Polym. Sci. Polym. Phys. Ed.*, **24**, 1695 (1986).
8. H. Muramatsu and W. R. Krigbaum, *J. Polym. Sci. Polym. Phys. Ed.*, **25**, 2303 (1987).
9. D. Done and D. G. Baird, *Polym. Eng. Sci.*, **27**, 816 (1987).
10. F. N. Cogswell, *Br. Polym. J.*, **12**, 170 (1980).
11. D. Acierno, F. P. La Mantia, G. Polizzotti, A. Ciferri, and B. Valenti, *Macromolecules*, **15**, 1455 (1982).
12. G. D. Butzbach, J. H. Wendorff, and H. J. Zimmerman, *Polymer*, **27**, 1337 (1986).
13. M.-Y. Cao and B. Wunderlich, *J. Polym. Sci. Polym. Phys. Ed.*, **23**, 531 (1985).
14. T.-S. Chung, *Polym. Eng. Sci.*, **26**, 901 (1986).
15. S. K. Varshney, *J. Macromol. Sci. Rev. Macromol. Chem. Phys.*, **C26**, 551 (1986).
16. G. W. Calundann and M. Jaffe, *The Robert A. Welch Foundation Conferences on Chemical Research, XXVI, Synthetic Polymers*, Houston, TX, Nov. 1982, pp. 247-287.
17. *Celanese Specialty Operations: Vectra, High Performance Resins*, a technical leaflet, Publication 196 B.
18. E. Suokas, J. Sarlin, and P. Törmälä, *Molecular Crystals and Liquid Crystals*, H. Gasparoux and F. Hardoion, Eds., Gordon and Breach, New York, 1988, to appear.
19. M. M. Denn, *Computational Analysis of Polymer Processing*, R. A. Pearson and S. M. Richardson, Eds., Applied Science, New York, 1984.
20. V. F.-M. Lu and J. E. Spruiell, *J. Appl. Polym. Sci.*, **23**, 1541 (1987).
21. A. Ziabicki and K. Kedzierska, *Kolloid Z.*, **171**, 51 (1960).
22. T. Ishibashi, K. Aoki, and T. Tshii, *J. Appl. Polym. Sci.*, **34**, 1541 (1987).
23. B. Tsoi, *Acta Polym.*, **38**, 453 (1987).
24. A. D. Gotsis and D. G. Baird, *J. Rheol.*, **29**, 539 (1985).
25. H. Sugiyama, D. N. Lewis, J. L. White, and J. F. Fellers, *J. Appl. Polym. Sci.*, **30**, 2329 (1985).
26. K. F. Wissburn, *Br. Polym. J.*, **12**, 163 (1980).
27. A. Ziabicki, *High Speed Fiber Spinning*, A. Ziabicki and H. Kawa, Eds., Wiley-Interscience, New York, 1985.
28. S. Kenig, *Polym. Eng. Sci.*, **27**, 887 (1987).
29. Y. Ide and Z. Ophir, *Polym. Eng. Sci.*, **23**, 261 (1983).
30. J. A. Cuculo and G.-Y. Chen., *J. Polym. Sci. Polym. Phys. Ed.*, **26**, 179 (1988).
31. L. C. Sawyer and M. Jaffe, *J. Mater. Sci.*, **21**, 1897 (1986).
32. J. L. White and Y. Ide, *J. Appl. Polym. Sci.*, **22**, 3057 (1978).
33. S. Kase, *J. Appl. Polym. Sci.*, **18**, 3279 (1974).
34. H. Ishihara and S. Kase, *J. Appl. Polym. Sci.*, **20**, 169 (1976).
35. H. J. Yoo, *Polym. Eng. Sci.*, **27**, 192 (1987).
36. G. F. Gruz-Saenz, G. J. Donnelley, and C. B. Weinberger, *AIChE J.*, **22**, 441 (1976).
37. A. B. Metzner and G. M. Prilutski, *J. Rheol.*, **30**, 661 (1986).
38. W. R. Krigbaum, C. K. Liu, and D.-K. Yang, *J. Polym. Sci. Polym. Phys. Ed.*, **26**, 1711 (1988).

Received April 12, 1989

Accepted July 13, 1989